

## ELM-induced cold pulses propagation in ASDEX Upgrade

E. Trier<sup>1</sup>, E. Wolfrum<sup>1</sup>, M. Willensdorfer<sup>1</sup>, Q. Yu<sup>1</sup>, F. Ryter<sup>1</sup>, C. Angioni<sup>1</sup>, M. G. Dunne<sup>1</sup>,  
S. Denk<sup>1,2</sup>, R. Fischer<sup>1</sup>, P. Hennequin<sup>3</sup>, B. Kurzan<sup>1</sup>, T. Odstrcil<sup>1,2</sup>, P. A. Schneider<sup>1</sup>,  
U. Stroth<sup>1,2</sup>, B. Vanovac<sup>4</sup>, the ASDEX Upgrade team, the EUROfusion MST1 Team<sup>5</sup>

<sup>1</sup> Max Planck Institute for Plasma Physics, D-85748 Garching, Germany

<sup>2</sup> Physik-Department E28, Technische Universität München, 85748 Garching, Germany

<sup>3</sup> Laboratoire de Physique des Plasmas, Ecole Polytechnique, CNRS,

F-91128 Palaiseau Cedex

<sup>4</sup> DIFFER - Dutch Institute for Fundamental Energy Research, Eindhoven, the Netherlands

<sup>5</sup> See Meyer et al. , Overview of progress in European Medium Sized Tokamaks towards an integrated plasma-edge/wall solution, accepted for publication in Nuclear Fusion

Understanding the electron heat transport in tokamaks is necessary to predict the performance of future fusion reactors. It has been shown that the edge region can have a strong impact on the overall confinement [1, 2]. In this contribution, the inward propagation of the electron temperature perturbations induced by Edge Localized Modes (ELM) is studied, using Electron Cyclotron Emission (ECE) measurements. A characterisation of the ELM-induced dynamics of the region (e.g.  $0.7 < \rho_{pol} < 0.95$ , where  $\rho_{pol}$  is the normalized poloidal radius) can reveal some features of the electron heat transport, and complement the understanding of the inter-ELM pedestal evolution.

In ASDEX Upgrade the electron temperature is measured by a 60 channels electron cyclotron emission (ECE) heterodyne radiometer, which detects the second harmonic extraordinary mode at  $|B_t| \sim 2.5$  T. The system consists of 24 channels with a spatial resolution of 12 mm, and 36 channels with a resolution of 5 mm at the edge. The sampling rate is 1 MHz; in this study the data is down-sampled to 8 kHz.

The penetration of ELM-induced cold pulses, subsequent to the initial electron temperature crash, is analysed in a database of 41 ASDEX Upgrade stationary H-mode Deuterium plasmas. Plasmas parameters are in the range  $I_p = 0.8 - 1.15$  MA,  $|q_{95}| = 3.5 - 7.6$ ,  $|B_t| = 2.45 - 2.68$  T, (low) triangularity  $\delta = 0.21 - 0.28$ , addi-

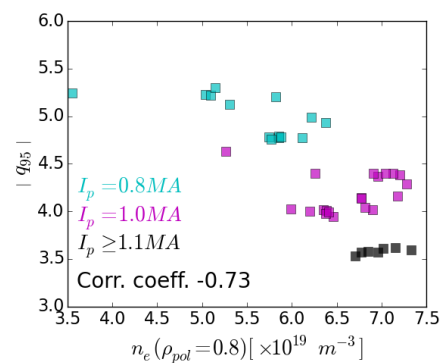


Figure 1: Position of the considered plasmas in the  $n_e(\rho_{pol} = 0.8) - |q_{95}|$  plane, where the electron density is measured by Thomson scattering.

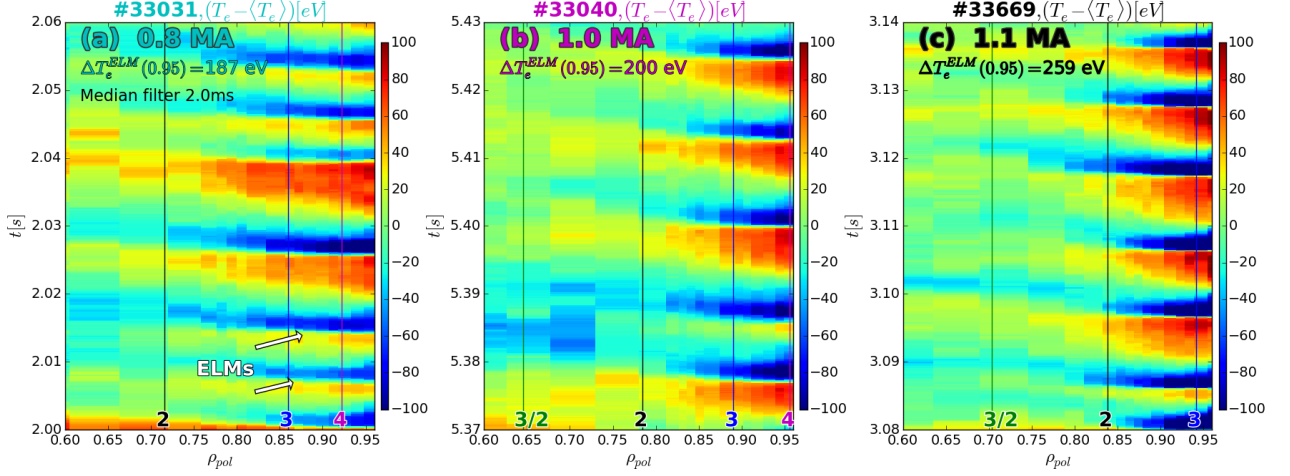


Figure 2: Color maps of typical  $T_e$  perturbation ( $T_e(\rho_{pol}, t) - \langle T_e \rangle(\rho_{pol})$ ) for 3 shots with  $I_p = 0.8, 1.0$ , and  $1.1$  MA, as a function of time and the time-averaged  $\rho_{pol}$ . The position of low-order rational surfaces is indicated by the vertical lines.

tional heating power  $P_{aux} = 2.6 - 13.9$  MW and electron density at  $\rho_{pol} = 0.8$  in the interval  $3.5 - 7.3 \times 10^{19} m^{-3}$ . No magnetic perturbations are applied during the considered time windows. Note that a correlation between  $I_p$  (or  $q_{95}$ ) and  $n_e$  is difficult to avoid in this dataset, since the 'natural' density is proportional to the plasma current [3], which is shown in figure 1.

In figure 2, the electron temperature perturbation induced by the ELMs is represented by color maps in the  $(\rho_{pol}, t)$  plane for 3 discharges with different plasma current ( $I_p = 0.8, 1.0$ , and  $1.1$  MA). The ELM-affected region is more extended at lower  $I_p$  (subfigure a): this is analysed in more detail in the remaining part of this contribution.

The penetration of ELM-induced cold pulses is quantified by considering the  $T_e$  radial decorrelation length, using as a reference an ECE channel at the pedestal top ( $\rho_{pol} = 0.95$ ). The radial profiles formed by the correlation with the reference channel are calculated for each discharges, by averaging a series of 10 time-windows of 200 ms. These profiles are plotted in figure 3.

A parameter designed as *ELM penetration radius* is introduced to quantify the ELM-induced cold pulse decay: it is defined here as the normalized poloidal radius for which the correlation with  $\rho_{pol} = 0.95$  drops to a value of 0.5. In figure 4a, this radius is compared with the radius of the  $q = 2$  surface, showing a strong link between the

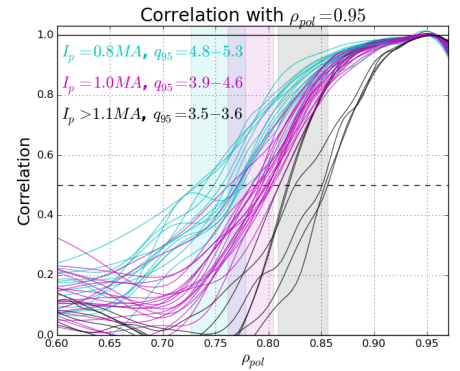


Figure 3: Radial profiles of correlation with channels at  $\rho_{pol} = 0.95$  for all discharges. Ranges of ELM penetration radius are shaded.

penetration of ELM-induced perturbations and the  $q$ -profile. Note that this plot is not sufficient to prove a special role played by the  $q = 2$  surface (the choice of a value of 2 for the safety factor, or of 0.5 for the correlation being arbitrary). However, it shows that the safety factor profile is playing a primary role in determining the propagation of ELM-induced  $T_e$  perturbations in this near-edge region. This is the main result of this contribution. It is completed in the next sections by considering other possible parameters that could also have influenced the ELM penetration, but are in fact of secondary influence: the edge electron density/pressure and the ELM strength.

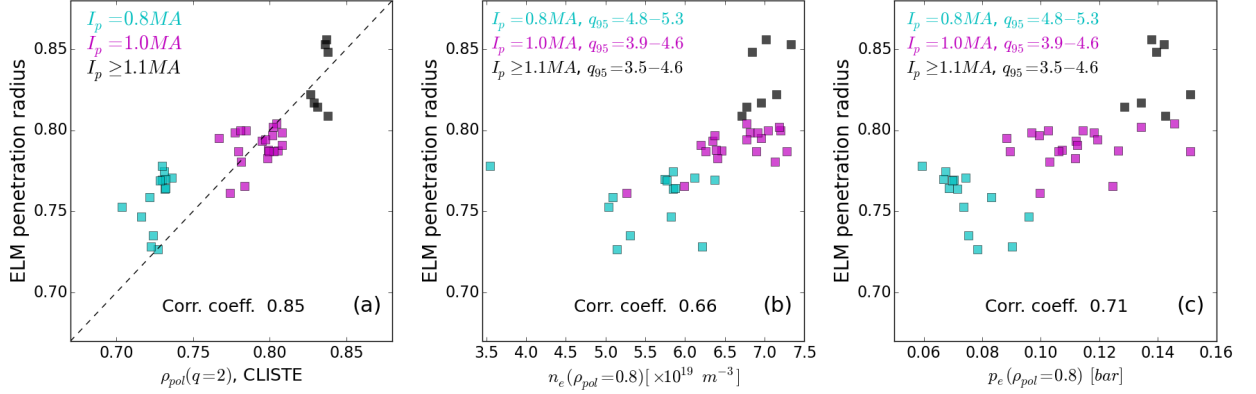


Figure 4: (a) ELM penetration radius as a function of the position of a given rational surface ( $q = 2$ ), (b) the edge electron density  $n_e(\rho_{pol} = 0.8)$  (c) or the edge electron pressure  $p_e(\rho_{pol} = 0.8)$ . The correlation coefficient between the two quantities is indicated.

As shown in figure 1, the edge density is correlated with the plasma current in this dataset (and the edge safety factor). It is then expected that the ELM penetration radius is also correlated with the edge density. This is shown in figure 4b: such a correlation exists, but is weaker in comparison with the influence of the safety factor in figure 4a. The correlation with the ELM penetration radius are 0.66 for the density and 0.85 for the  $q = 2$  surface position. Similarly, the correlation between the penetration radius and the edge pressure  $p_e(0.8)$  is 0.71. The influence of the edge electron density or pressure on ELM penetration cannot be excluded, but should be of less importance than the  $q$ -profile.

The ELM strength would appear as a natural candidate to explain the differences in ELM-induced cold pulse penetration. It can be quantified by several quantities, which are considered in figure 5: the median value of the ELM-induced  $T_e$  drop at the pedestal top ( $\rho_{pol} = 0.95$ ), noted  $\Delta T_e^{elm}$  (subfigure a), the ELM-induced drop of plasma energy  $\Delta W_{MHD}^{elm}$  (subfigure b) or its relative variation  $\Delta W_{MHD}^{elm}/W_{MHD}$  (subfigure c). As indicated by the low correlation between these parameters and the ELM penetration radius, the ELM strength is not the main explanation for the variation in cold pulse penetration. An interesting observation in subfigure (a) and (b) is that at larger plasma current, the ELM penetration is more shallow in spite of the generally

stronger absolute drop in plasma energy and edge  $T_e$ .

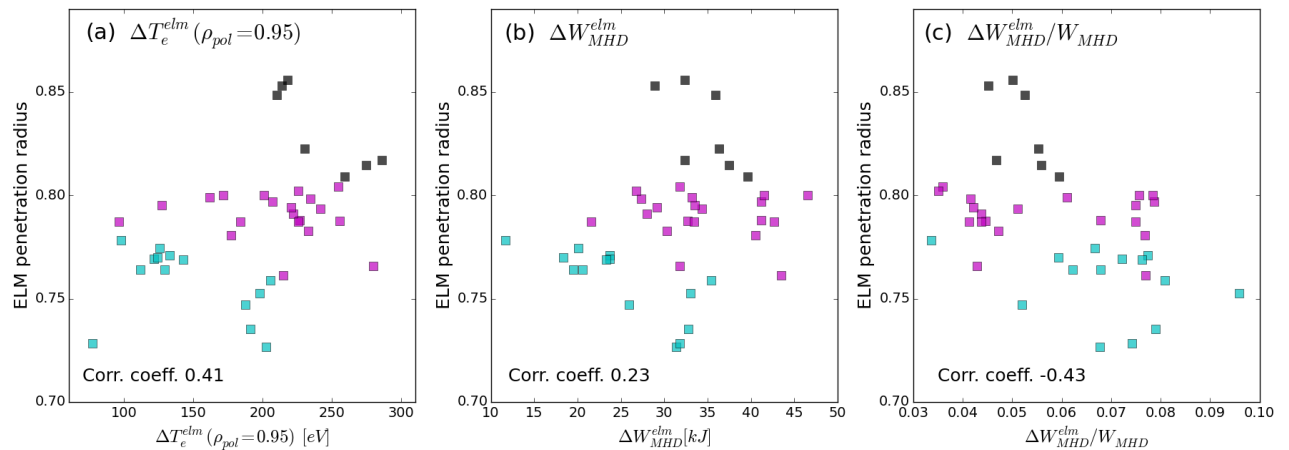


Figure 5: ELM penetration radius as a function of the median values of: (a) the ELM-induced  $T_e$  drop at  $\rho_{pol} = 0.95$ , noted  $\Delta T_e^{elm}$ , (b) the drop of plasma energy  $\Delta W_{MHD}^{elm}$ , (c) the relative drop  $\Delta W_{MHD}^{elm}/W_{MHD}$

The influence of other global ( $P_{aux}$ ) or local ( $\rho^*$ ,  $v^*$ ,  $\beta$ ) parameters have also been tested. Their correlation with the ELM penetration radius is lower than with the parameters shown in figure 4:  $\rho_{pol}(q=2)$ ,  $n_e(\rho_{pol}=0.8)$  or  $p_e(\rho_{pol}=0.8)$ . Note that the plasmas from this dataset have a moderate triangularity  $\delta < 0.28$ . A different behaviour is observed at higher  $\delta$ , that is subject to ongoing analyse.

An ELM-induced inward displacement of the whole plasma would be seen as a decrease in  $T_e$  affecting simultaneously all the ECE channels on the low field side: this effect is not detected in this dataset and should be negligible in comparison with the 'real'  $T_e$  perturbation.

In summary, the inward propagation of the ELM-induced cold pulses is strongly affected by the safety factor profile. Interestingly, with increasing plasma current the ELM penetration is more shallow in spite of the stronger ELMs. An open question would be whether this is due to phenomena related with the ELMs (e.g. transient islands or stochastic layers), or more universal features of the electron heat transport in the corresponding near-edge region: for example an influence of the plasma current has been reported in TCV L-mode plasmas [2].

## References

- [1] W. Suttrop et al., Plasma Phys. Control. Fusion **39** 2051 (1997)
- [2] O. Sauter et al., Physics of Plasmas **21**, 055906 (2014)
- [3] M.J. Greenwald, Plasma Phys. Control. Fusion **44** R27 (2002)

## Acknowledgements

This work has been carried out within the framework of the EUROfusion Consortium and has received funding from the Euratom research and training programme 2014-2018 under grant agreement No 633053. The views and opinions expressed herein do not necessarily reflect those of the European Commission.